Terrigenous sedimentation of the upper Quaternary in the Cayar deep-sea fan (Senegal-Gambia abyssal plain-Atlantic Ocean)

Upper Quaternary
Hemipelagic sedimentation
Turbiditic sedimentation
African margin
Atlantic Ocean

Quaternaire supérieur
Sédimentation hémipélagique
Sédimentation turbiditique
Marge africaine
Océan Atlantique

Guy L. KOUNKOU, Jean-Paul BARUSSEAU
Laboratoire de Recherches de Sédimentologie Marine, Université de Perpignan, avenue de Villeneuve, 66025 Perpignan, France.

Received 14/2/87, in revised form 25/3/88, accepted 4/4/88.

ABSTRACT

The results of a sedimentological and micropaleontological study of a core taken from the Cayar deep-sea fan are presented in order to define the chronology and the processes of deposition.

Hemipelagic and turbiditic inputs are separated from lithological, micropaleontological and isotopic characteristics. A condensed stratigraphic column including only the hemipelagic component is then compared—from a carbonate and isotopic point of view—with other distributions available in the region. The lower part of the core bottoms in isotopic stage 5.

The hemipelagic component is generally constant, except in the Holocene, where sedimentation rates are about three times greater than in preceding times. Turbiditic occurrences, abundant in all the stages, seem to be more frequent during the cold-to-warm transitions (arid to humid) coinciding with the transgressive glacio-eustatic sequences. However the Holocene displays a greater occurrence of turbidite layers with the shortest recorded periods.

Oceanol. Acta, 1988, **11**, 4, 359-368.

RÉSUMÉ

Sédimentation terrigène au Quaternaire supérieur dans le delta sous-marin de Cayar (plaine abyssale de Sénégal-Gambie, Océan Atlantique)

Une carotte de l'éventail détritique profond de Cayar, située en contrebas de la marge sénégalaise et de la ride du Cap-Vert, a fait l'objet d'une étude sédimentologique et micropaléontologique, en vue de définir la chronologie des dépôts et les types de contribution sédimentaire. On a cherché, dans un premier temps, à dégager le signal purement hémipélagique, de façon à obtenir un enregistrement non perturbé par les alternances parasites des nombreuses venues turbiditiques qui constituent l'essentiel des 10,20 m de la carotte. Le signal — carbonates, $\delta^{18}O$, $\delta^{13}C$ — a été confronté aux courbes, étalonnées en temps, disponibles dans la région et permet d'établir un cadre temporel remontant à l'intérieur du stade isotopique 5. Les taux de sédimentation du matériel hémipélagique dénotent une relative constance, sauf au cours de l'Holocène où ils sont multipliés par un facteur 3. Les occurrences turbiditiques ont, dans un second temps, été caractérisées. L'analyse granulométrique permet de mettre en évidence les changements de texture imputables aux variations d'activité des courants de turbidité. Un ensemble de 43 turbidites est ainsi repéré. Ces venues terrigènes s'observent dans tous les stades, et semblent plus fréquentes lors des transitions froid-aride à chaud-humide, c'est-à-dire au début des poussées transgressives. Là encore, la sédimentation turbiditique est favorisée à l'Holocène.

Oceanol. Acta, 1988, **11**, 4, 359-368.

INTRODUCTION

Core 16401-4 was recovered on the upper deep-sea fan of Cayar submarine valley (Senegal-Gambia abyssal plain; Fig. 1) during the Geotropex 83 cruise of *FS Meteor* (Sarnthein *et al.*, 1983). Sediments deposited in this kind of sedimentological setting are generally varied in origin and partly redeposited. However, turbidites may be absent from pelagic layers formed over sufficiently long intervals of time (Piper, Normark, 1983).

Because of the interspersed hemipelagic input into the turbiditic background, it is not easy to determine chronological limits by comparing usual signals, provided by carbonate content, distribution of foraminifers and isotope analysis, with reliable records available in the region (Ericson *et al.*, 1961; Damuth, 1975; Pflaumann, 1975; Gardner, Hays, 1976; Ruddiman, McIntyre, 1976; Berggren *et al.*, 1980; Crowley, 1983; Sarthein *et al.*, 1984).

In this paper, we have tried to emphasize criteria which separate the relatively few layers of pelagic sediment from the predominant turbidite deposits, in order to obtain a condensed stratigraphic column composed only of pelagic layers. This sequence of "normal" pelagic sedimentation was then divided into stages by comparing carbonate content and isotopic curves. The number of turbiditic events for each stage and their average periodicity were then computed.

STUDIED AREA AND METHODOLOGY

The Cayar deep-sea fan is located 300 km west of Cap Vert (Senegal), a continental margin with a rather narrow shelf and a slope considerably influenced by the impingement of the Cabo Verde rise. Core 16401-4 was recovered at the outlet of the canyon channel on the northern flank of the main fan valley, which is an element of a complex system of distributary channels that abruptly bends in that part of the upper fan from 60° to a final direction of 170°. Core 16401-4 is 10.20 m long. Samples are generally collected every 10 cm and the following analyses were performed: $CaCO_3$ content, determined from 1 g of sediment; pelitic (<40 μm) and arenic (>40 μm) indices; fine sediment grain-size by the

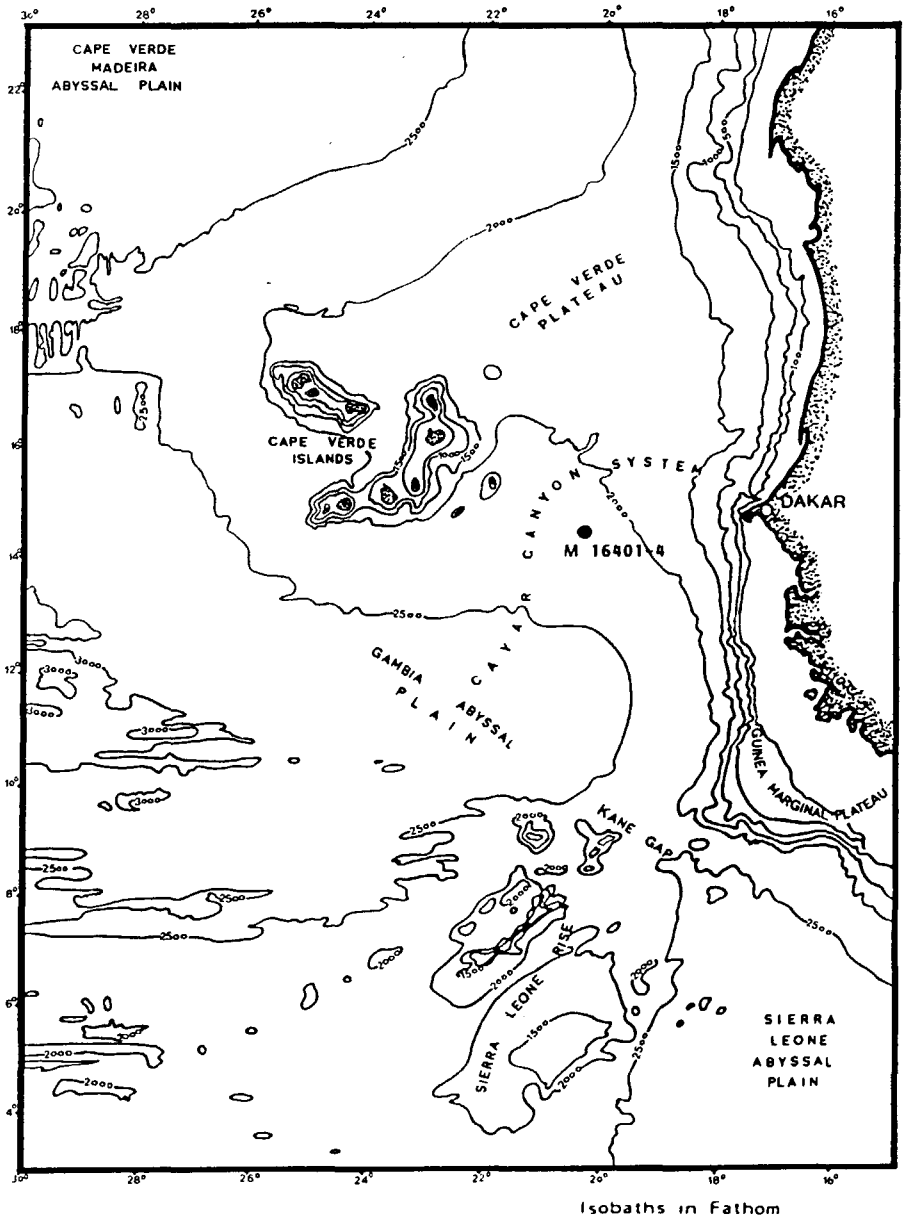

Figure 1

Location of "Geotropex" M. 16401-4 core in the Senegal-Gambia abyssal plain.

Localisation de la carotte M. 16401-4 (plaine abyssale de Sénégal-Gambie; mission Géotropex).

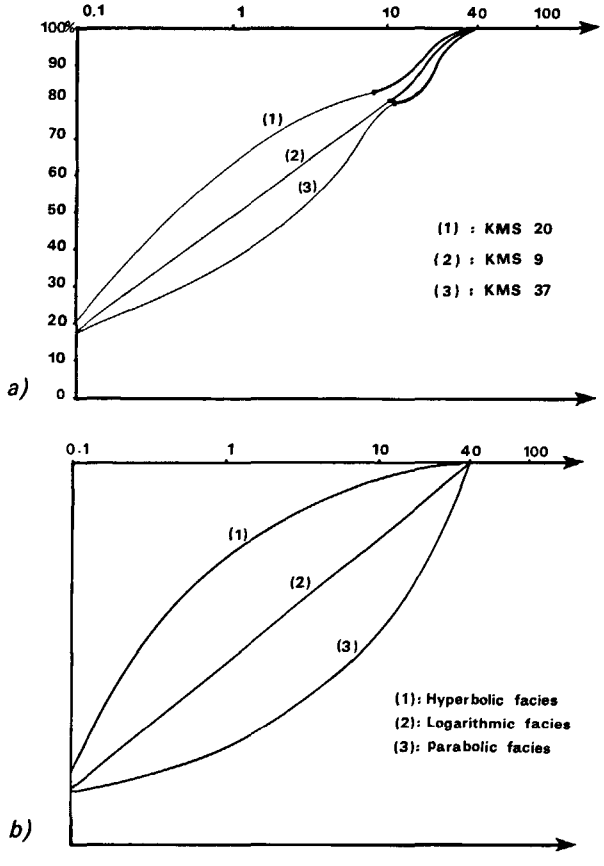

Figure 2

Method of grain-size analysis.
A) Three actual cases of grain-size. In every case, the silt population (thick-line) is combined with a fine grain-size tail (thin-line). The limit between the two populations is marked with a spot, which is located between 2 and 12 μm.
B) Grain-size facies of fine sediments (from Rivière, 1952).

Méthode d'analyse granulométrique.
A) Trois exemples de granulométrie. Dans chaque cas, la population silt (ligne épaisse) est associée à une queue de distribution fine (ligne mince). La limite entre les deux distributions est notée par un point, localisé entre 2 et 12 μm.
B) Faciès granulométrique des sédiments fins (d'après Rivière, 1952).

pipette method and sand grain-size by sieving; visual qualitative and quantitative evaluation of elements (in particular microfaunal assemblages). In addition, $\delta^{18}O$ and $\delta^{13}C$ were measured by R. Zahn at the C-14 laboratory of the Christian Albrecht University (Kiel).

COMPOSITION OF THE CONDENSED STRATIGRAPHIC COLUMN

The distinction between pelagic and turbiditic layers is established in relation to the grain-size structure of each sample and the nature of microfaunal assemblage.

Grain-size structure of sediments

Most sediments evince a close association of a silt, occasionally sand, population and a fine tail starting from 2-12 μm (Fig. 2A). Silt population is usually unimodal (60 cases out of 62), and can be described by using standard grain-size indices (position, sorting). However skewness was not assessed, due to the uncertainty about the link with the fine fraction. The fine tail can display a "grain-size facies" (Rivière, 1952) which depends on: 1) an enrichment of very fine particles (<1 μm): "hyperbolic facies"; 2) the presence of rather "coarse" fine particles (1 to 6 μm): "parabolic facies"; 3) the lack of any sorting: "logarithmic facies" (Fig. 2B). As shown by Kranck (1984), the size distribution of a bottom sediment resulting from a turbidity current may be seen as a two-component mixture of two sub-populations, the coarser one of which may disappear. One of the sub-populations is the fine tail reported here and the other is the silt population. In the present study, the fine tail is associated with silt populations in 60.8% of the cases, in a strongly negatively skewed distribution. The silt population is prominent (with a coarse silt to fine sand assemblage higher than 50%) in 12.9% of these cases. In 29.2% of the layers, only the fine tail exists without any trace of silt population; the aspect of the grain-size curves is then parabolic (excess of "coarse" fine particles), logarithmic, or hyperbolic (excess of very fine particles), as shown in Table 1.

Figure 3

I_o *vs. silt population content (triangles) and vs. clay population content (open circles).*

Diagramme i_0/teneur en population silt (triangle) et i_0/teneur en population argile (cercles).

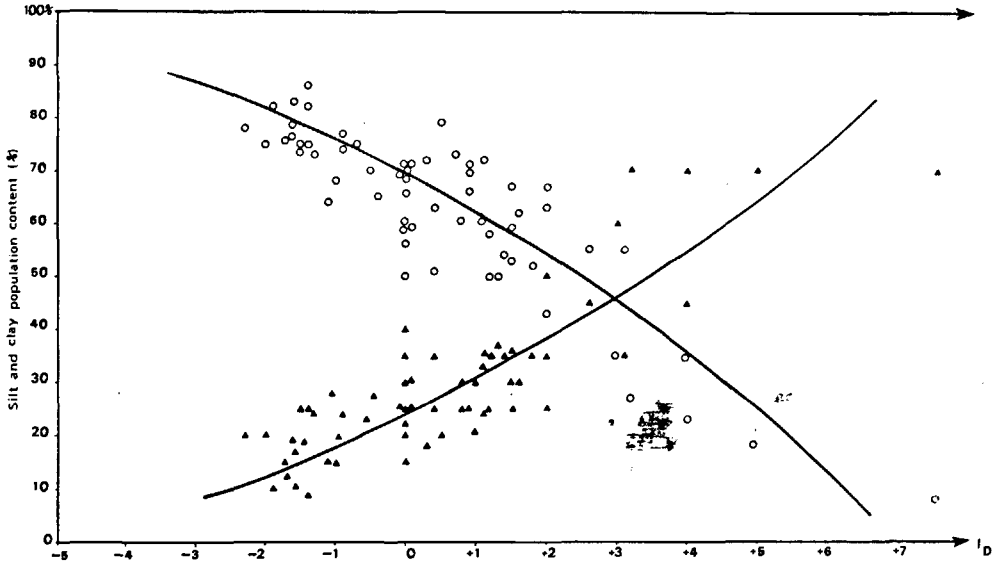

Table 1

Mode and finest grain of the silt population, silt content (%) and grain-size facies of the fine part of the sediment. H: hyperbolic facies of the fine sediment; L: logarithmic facies of the fine sediment; P: parabolic facies of the fine sediment; SH: mixing of a silt well-sorted sigmoidal population (S) with a hyperbolic facies of the finest population (H); SL: mixing of a silt well-sorted sigmoidal population (S) with a logarithmic facies of the finest population (L); SP: mixing of a silt well-sorted sigmoidal population (S) with a parabolic facies of the finest population (P).

Mode et grain le plus fin de la population silt, teneur en silt (%), faciès granulométrique de la partie fine du sédiment.
H, faciès hyperbolique; L : faciès logarithmique; P : faciès parabolique; SH : mélange d'une population silt sigmoïdale bien triée (S) et d'un faciès hyperbolique (H); SL, SP : idem avec un faciès logarithmique (L) ou parabolique (P).

Sample No.	Mode	Finest grain	Silt population (%)	Grain-size facies	Sample No.	Mode	Finest grain	Silt population (%)	Grain-size facies
1				H	56				P
2	34	5	42	SH	57	21	10	31	SH
3				P	58	16	4	33	SH
4				H	59	46	20	24	SL
5				L	60	27	5	73	SH
6	11	5	18	SH	61				P
7				L	62				L
8				H	63	17	4	24	SH
9	12	4	23	SL	64	20	7	24	SH
10				H	65	21	7	43	SH
11				H	66	8	3	22	SH
12	24	11	23	SH	67				H
13	9	3	22	SH	68	11	7	23	SH
14				L	69				L
15				H	70				L
16	9	2	28	SH	71				L
17				L	72				H
18	25	12	30	SL	73	38	2	90	SL
19	21	6	52	SL	74	22	5	28	SH
20	16	4	24	SH	75	23	7	14	SH
21	8	3	19	SH	76	18	5	28	SH
22	6	3	18	SH	77				L
23				L	78	20	7	35	SL
24	17	5	29	SH	79	28	10	68	SL
25	9	4	18	SH	80				P
26	11	5	17	SH	81				P
27	17	4	32	SH	82	14	6	22	SH
28	20	9	28	SH	83				H
29	15	5	33	SH	84	17	7	28	SH
30	19	11	27	SH	85				L
31	18	5	30	SH	86				L
32				L	87	16	5	22	SH
33	13	4	23	SH	88				H
34-35				H	89				L
36	19	4	25	SP	90	15	8	18	SH
37	22	12	20	SP	91	38	7	72	SH
38	17	3	45	SP	92	21	5	38	SP
39	14	4	35	SH	93	28	16	16	SH
40				H	94	17	12	14	SH
44	19	5	36	SH	95				H
45				H	96				P
46	25	3	44	SH	97				H
47	12	3	26	SH	98	13	4	33	SH
48	22	5	40	SP	99	30	5	60	SH
49				P	100	24	12	24	SH
50				P	101				L
51	22	6	34	SH	102	60	3	92	SL
52	33	5	72	SH	103	16	3	35	SH
53	13	4	33	SH	104	14	5	34	SH
54				P	105	51	24	45	SL
55	22	4	42	SL	106				H

The build-up of a clearly individualized silt population with a sigmoidal curve is a meaningful index of the action of a transport process. Moreover, 96.8% of the layers presenting such a population give evidence of a gaussian grain-size structure in the range 2-12 to 40-300 μm. The larger sensitivity of the silt population to hydrodynamic effects is clearly disclosed when comparing its abundance to the index i_o (computation of i_o is described in detail in Martin *et al.*, 1981) which denotes the transport and sorting activities. The silt population content increases when i_D increases (Fig. 3) while clay content (<2 μm) decreases. Hence, an individualized gaussian population betrays the existence of a sorting agent acting on a set of grains during the transport phase, and rules out the possibility of grain-by-grain sedimentation. This observation is consistent with the sedimentological background at the outlet of the Cayar canyon where the occurrence of active hydrosedimentological processes may be presumed.

Consequently, the presence of a silt assemblage displaying a gaussian structure of the grain-size was considered as a first criterion (step 1) to distinguish the turbiditic layers (Fig. 4). Unfortunately, the converse is not true and the absence of a clear silt population does not mean that no mass-transport occurred. Three kinds of deposition processes can theoretically lead to grain-size distributions with no silt component: 1) pelagic sedimentation; 2) terminal and distal sedimentation of a turbidity current; 3) reworking of earlier pelagic sediments in the slope by a turbidity current.

Distinction of pelagic layers

Among the 40 layers where the absence of silt provides sure evidence of transport, the microfaunal (foraminifers) assemblage was examined in order to discard those for which a shallow origin may be surmised. Two criteria were used: the relative content of benthic foraminifers vs. pelagic forms (Faugères *et al.*, 1981) and the presence of shelf-originated species (Griggs, Kulm, 1970: *Nonionella turgida, Ammonia beccarii, Nonion asterizans, Cibicides lobatulus, C. refulgens, Triloculina trigona* were considered as the main shelf-derived benthic species (Blanc-Vernet, 1967).

Table 2 contains these data for all the layers and Figure 5 presents the distribution of the pairs of values for each sample. Clearly, the distinction between layers with or without a silt population is not obvious from this point of view. One of the reasons why benthic and even shallow benthic foraminifers occur in the hemipelagic sediments is the ability of their tests to be transported more easily than coarse silt. Consequently, the shelf benthic foraminifer assemblage shown in some layers cannot be taken as an absolute indicator of turbiditic transport. However, the heavy line separated an upper field where relatively high values of shallow species and/or relatively high values of the benthic-pelagic ratio are observed. This new criterion (step 2) for distinguishing between the two kinds of deposition allows us to discard six more layers from the hemipelagic record (Fig. 4).

The remaining layers were used to build a first set of curves gathering $\delta^{18}O$, $\delta^{13}C$ (on *Globigerinoides sacculifer* tests) and carbonate (on the bulk sediment) signals (Fig. 6). Comparison of the most pertinent data ($\delta^{18}O$ and carbonate) with similar information in the region (Hays, Perruzza, 1972; Gardner, Hays, 1976; Sarnthein *et al.*, 1982; 1984; Crowley, 1983; Lutze *et al.*, 1986; Mienert, 1986; Pflaumann, 1986) shows a lack of homogeneity in the results. For instance, it is impossible to correlate chronological limits of isotopic and carbonate stages. Among the 34 layers, 9 samples do not

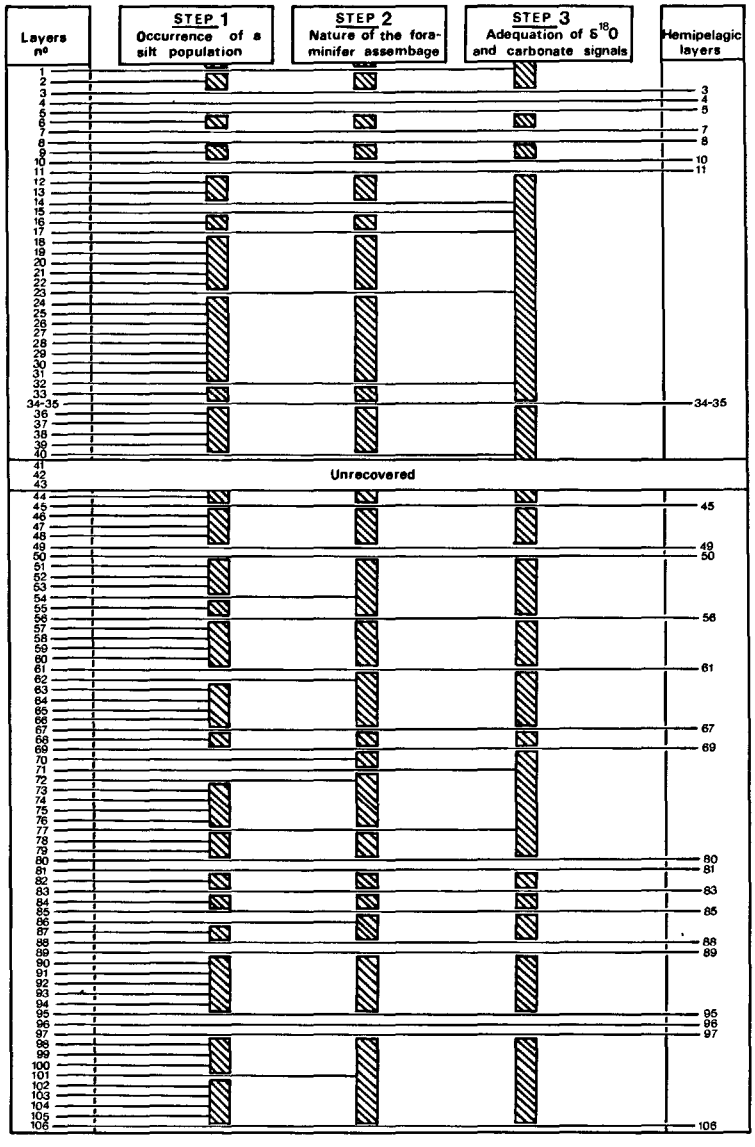

Figure 4

Set of criteria used to define the pelagic and turbiditic layers in the core M. 16401-4.

Critères utilisés dans la définition des niveaux pélagiques et turbiditiques de la carotte M. 16401-4.

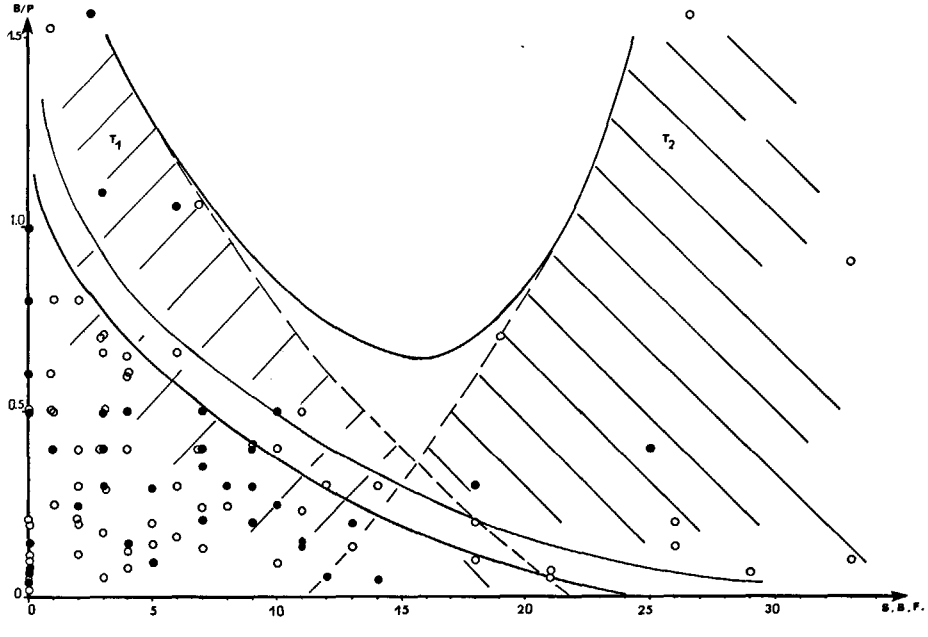

Figure 5

Percentages of the shallow benthic foraminifers (SBF) vs. the relative content benthic/pelagic foraminifers (B/P). Open circles: from samples with a silt population; black circles: from samples without a silt population; T1: turbidites with reworked hemipelagic sediment; T2: turbidites from the upper continental slope.

Diagramme pourcentage en foraminifères benthiques peu profonds (SBF)/teneur relative benthiques-pélagiques (B/P). Cercles vides : échantillons à population silt; cercles pleins : échantillons sans population silt.

Table 2
General results obtained from the study of the core M. 16401-4.
Résultats généraux de l'étude de M.16401-4.

Sample No.	$\delta^{18}O$*	$\delta^{13}C$*	$CaCO_3$	B/P (%)	Shallow Benthic (%)	Sample No.	$\delta^{18}O$*	$\delta^{13}C$*	$CaCO_3$	B/P (%)	Shallow Benthic (%)
1			17.14	0.6	0	54	0.81	2.03	7.02	1.08	3
2	−0.30	2.20	17.00	0.05	0	55	0.69	1.90	2.76	0.64	3
3	−0.79	2.37	16.22	0.5	3	56	0.62	1.57	8.51	0.98	0
4	−0.03	2.13	19.30	0.6	0	57	0.36	1.47	7.66	2.6	1
5	−0.52	2.35	18.00	0.3	3	58	0.67	2.36	9.36	0.7	3
6	−0.48	2.25	20.00	0.2	0	59	0.83	1.84	11.00	0.5	3
7	−0.82	2.46	22.00	0.04	0	60			8.27	11.5	27
8	−0.75	2.23	22.41	0.06	14	61	0.60	2.37	8.72	0.8	0
9	−0.36	2.39	9.57	0.2	2	62	0.16	2.21	2.54	2.4	2
10	−0.29	2.28	9.54	0.4	1	63			9.08	0.66	4
11	−0.43	2.33	9.18	0.06	12	64	0.93	1.61	12.21	0.5	0
12	−0.27	2.16	23.00	0.1	18	65	0.03	1.42	7.79	0.2	26
13	−0.33	2.26	4.89	0.2	2	66			8.72	0.4	3
14	−0.33	1.98	2.76	0.3	5	67	0.95	1.81	6.80	0.12	5
15	−0.06	1.65	8.29	0.25	2	68	0.65	2.04	10.81	0.7	3
16	0.19	1.72	8.72	0.3	2	69	1.08	1.79	9.79	0.4	7
17	0.06	1.90	8.29	0.3	8	70	0.29	2.13	7.23	0.5	10
18	−0.17	2.03	7.68	0.4	7	71	0.31	1.75	11.24	0.16	4
19	0.18	1.84	7.44	0.4	4	72	0.22	1.68	10.00	0.4	25
20	0.16	1.81	19.50	0.12	0	73	−0.29	2.06	12.51	0.9	33
21	0.15	2.15	5.10	0.3	3	74	0.05	2.04	14.00	0.43	9
22	−0.05	1.91	7.23	0.2	18	75	0.01	2.40	14.52	0.15	5
23	0.19	2.14	5.96	0.3	9	76	0.55	1.85	11.10	0.06	3
24	−0.21	2.01	8.93	0.3	14	77	0.54	1.60	7.00	0.16	11
25			19.00	0.07	4	78			5.55	0.08	21
26	0.48	1.88	8.93	0.2	5	79	1.01	1.68	12.21	0.27	8
27	0.56	1.80	8.29	0.2	0	80	0.56	2.14	17.30	0.22	7
28	0.73	1.44	7.63	0.12	2	81	0.18	2.39	19.30	0.35	7
29	0.50	1.57	7.87	0.35	1	82	0.57	1.85	20.35	0.18	3
30	0.39	1.61	6.19	0.4	2	83	−0.04	2.08	12.40	0.14	0
31	0.17	1.29	7.87	0.02	0	84	0.51	2.08	13.10	0.09	33
32	0.92	1.72	16.00	0.08	0	85			15.53	0.4	9
33	0.95	1.76	7.44	0.5	1	86	0.08	2.05	10.35	0.3	18
34-35	1.09	2.06	5.10	0.6	1	87	0.09	2.10	10.53	0.3	12
36	0.93	1.79	8.08	0.12	4	88	−0.03	2.29	15.16	0.22	9
37	1.14	1.98	20.35	0.1	0	89	0.14	2.05	11.60	0.15	11
38	1.05	2.34	7.44	0.6	1	90	0.33	1.66	13.00	0.08	10
39	0.75	2.12	9.36	0.14	7	91	0.59	2.01	13.22	0.14	6
40	1.23	1.71	15.00	0.5	4	92	0.57	1.94	6.00	0.06	29
41						93	0.22	1.83	13.00	0.5	11
42			Unrecovered			94	0.28	1.91	14.00	0.14	26
43						95	−0.05	2.28	15.00	0.25	10
44	0.80	2.21	12.30	0.23	7	96	0.32	2.07	18.00	0.5	7
45	1.53	2.72	6.59	0.06	0	97	0.36	2.18	15.00	0.2	13
46	0.85	2.25	14.00	0.15	13	98	0.16	2.23	22.00	0.7	19
47	1.07	2.06	10.21	0.06	21	99	0.09	2.02	17.00	0.23	11
48	0.32	1.95	6.57	0.8	1	100	0.07	1.95	21.00	0.4	10
49	1.38	2.40	7.66	0.4	3	101	−0.13	1.98	18.00	1.04	6
50	0.94	2.16	11.00	0.5	0	102	0.63	1.44	9.51	0.3	6
51			8.69	0.56	4	103	0.44	1.58	13.23	0.5	1
52	0.46	2.23	7.87	1.08	7	104	0.07	1.86	15.00	0.8	2
53			8.29	0.66	6	105	0.24	1.81	12.30	0.6	4
						106	−0.14	1.72	15.00	0.3	3

*Measurements by R. Zahn (C 14 laboratory, Christian Albrecht-Univ., Kiel).

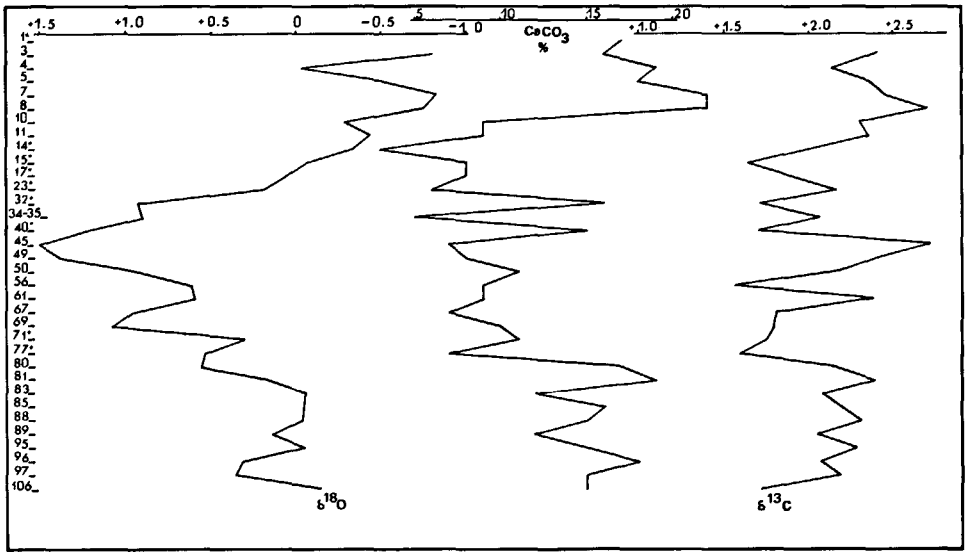

Figure 6
$\delta^{18}O$, $\delta^{13}C$ and carbonate variations along the 34 layers resulting from step 1 and step 2. The numbers with a star were eliminated from the log after the step 3.
Variations de $\delta^{18}O$, $\delta^{13}C$ et carbonates dans les 34 niveaux ayant franchi les filtres 1 et 2. Les numéros marqués d'une astérisque ont été éliminés à l'issue de l'étape 3.

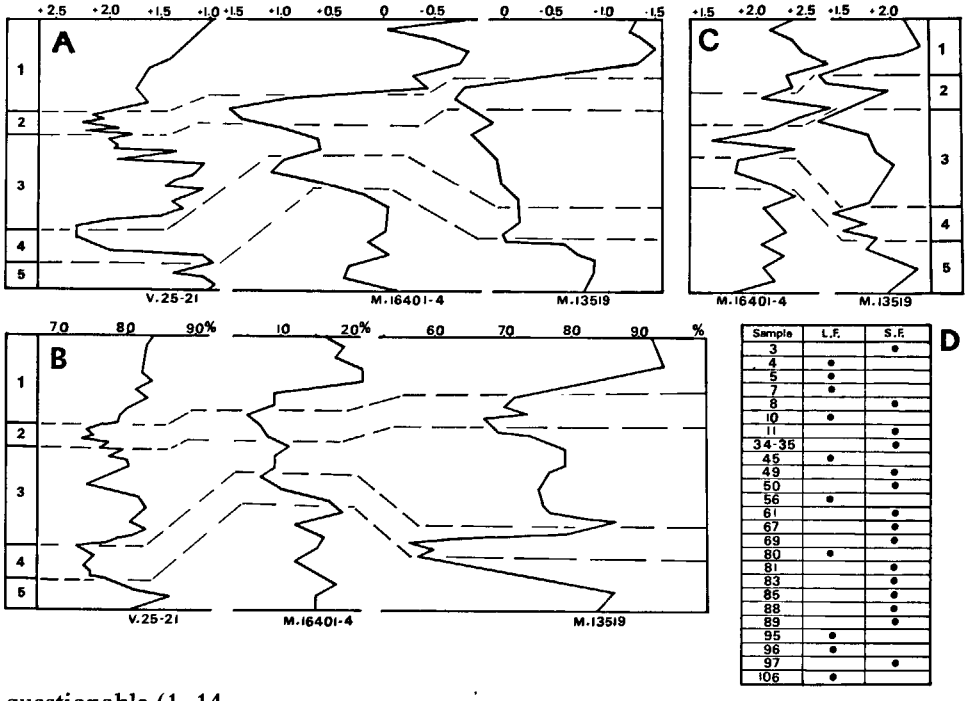

Figure 7
Comparison of $\delta^{18}O$ (A), $CaCO_3$ (B), $\delta^{13}C$ (C) and foraminifer size (D) between M. 16401-4, M. 13519 and V.25-21.
Comparaison de $\delta^{18}O$ (A), $CaCO_3$ (B), $\delta^{13}C$ (C) entre M.16401-4, M. 13519 et V. 25-21 et taille des foraminifères (D).

correctly match the curves and are questionable (1, 14, 15, 17, 23, 40, 71 and 77). Layer 1 displays a high value of $\delta^{18}O$ which is not established in the region (Crowley, 1983; Lutze *et al.*, 1986; Mienert, 1986). The very low $\delta^{18}O$ values of layers 45 and 49 and, to a lesser extent, of layers 34/35 are the clear signature of isotopic stage 2; the high carbonate contents of 32 and 40 must, therefore be ruled out as they do not compare well with the reference records for this stage (Fig. 7). In the same way, following the extrema observed in the cold stage 2, there is no convenient match for layers 14, 15, 17 and 23 between the measured isotopic O values, the observed low carbonate contents and their variations in V25-21 and M 13519. Because of this disagreement, these layers were discarded.

The case of layers 71 and 77 is not so obvious. Indeed, the $\delta^{18}O$ values found seem too small for an effective comparison with the cold conditions of stage 4. But in V25-21, at the bottom of stage 4, low $\delta^{18}O$ values are registered and simultaneously low carbonate contents occur. The two signals are out of phase. In spite of the uncertainty due to leads and lags of the signal variations in this stage, there is only one peak value in V25-21 as well as in M 13519. For this reason layers 71 and 77 were also dismissed.

Finally, as a result of this third step, 25 layers were passed through the successive filters. The hemipelagic beds are defined by a material: 1) whose dimensional assemblage of particles does not display any grain-size organization; 2) characterized by low percentage of benthic and shallow foraminifers; and 3) showing good agreement in successive $\delta^{18}O$ and/or carbonate values with the variations observed in the region.

In so far as the sampling recovered only 10% of the sedimentary column (1 cm every 10 cm), continuity of the "normal" pelagic sedimentation of the late Quaternary record sampled may not be thoroughly illustrated. However, due to the location of the site in the upper deep-sea fan, the prominence of the turbiditic influx is not disputable. Accordingly the 25 layers of the condensed column represent a proxydata to the normal pelagic sedimentation.

Chronology of deposition

The condensed stratigraphic column has the advantage of providing signals devoid of turbiditic background. Direct comparison may be made with information provided by other sites. Figure 7 shows the results relative to carbonate content and $\delta^{18}O$ and $\delta^{13}C$ ratios, compared with similar results from the Sierra Leone rise (Sarnthein *et al.*, 1984) and the Cabo Verde rise (Crowley, 1983). Carbonate content and oxygen-isotope (Fig. 7A and 7B) give a good correlation and provide a time framework. Core 16401-4 bottomed in stage 5. Stages 1 and 5 are well represented but only three layers are present in stage 3. The sedimentation rate of the pelagic input has been computed (Tab. 3). The deposition rate assessed for stage 5 is only an approximation since the age of the core-bottom sediments is not known. There is an increase by a factor of 2 to 5 in the Holocene sedimentation rate.

The vertical distribution of foraminifer sizes (Fig. 7D) compares fairly well with the chronological limits. Large foraminifers are more frequent in the "hyperthermal" (Van Zinderen, 1968) stages 1 and 5. However the marked change between layers 89 and 95 may reflect a climatic deterioration during substages 5d-a. The

Table 3
Sedimentation rate of the hemipelagic input.
Taux de sédimentation de la composante hémipélagique.

Isotopic stages	Thickness (mm)	Pelagic sedimentation rate ($mm.ky^{-1}$)
1	700	64
2	270	16
3	300	9
4	300	23
5	1050	$21 < s < 30$

Table 4

Mode, sorting index and content of the silt population; grain-size facies of the fine part of the sediment and grading of the turbiditic layers.
Mode, indice de triage et teneur en population silt ; faciès granulométrique de la composante fine et granoclassement des niveaux turbiditiques.

1	2	3	4	5	6
1				H	
2	34	1.54	42	SH	
6	11	1.54	18	SH	↑
9	12	1.54	23	SL	
12	24	1.20	23	SH	
13	9	1.70	22	SH	
14				L	↑
15				H	
16	9	1.54	28	SH	
17				L	↑
18	28	1.12	30	SL	
19	21	1.16	52	SL	
20	16	1.57	24	SH	
21	8	1.35	19	SH	↓
22	6	1.45	18	SH	
23				L	
24	17	1.32	29	SH	
25	9	1.62	18	SH	↑
26	11	1.41	17	SH	
27	17	1.37	32	SH	
28	20	1.41	28	SH	
29	15	1.41	33	SH	↑
30	19	1.18	27	SH	
31	18	1.45	30	SH	
32				L	↑
33	13	1.56	23	SH	
36	19	1.40	35	SP	
37	22	1.16	20	SP	↓
38	17	1.49	45	SP	
39	14	1.42	35	SH	
40				H	
		UNRECOVERED			
44	19	1.34	36	SH	
46	25	1.70	44	SH	↑
47	12	1.47	26	SH	
48	22	1.26	40	SP	
51	22	1.43	34	SH	↑
52	33	1.07	72	SH	
53	13	1.31	33	SH	
54				P	↑
55	22	1.62	42	SL	
57	21	1.15	31	SH	
58	16	1.58	33	SH	↑
59	46	1.35	24	SL	
60	27	1.15	73	SL	
62				L	↑
63	17	1.28	24	SH	
64	20	1.33	24	SH	↑
65	21	1.24	43	SH	
66	8	1.57	22	SH	
68	11	1.49	23	SH	
70				L	↑
71				L	
72				H	
73	38	1.25	90	SL	
74	22	1.40	28	SH	
75	23	1.50	14	SH	↑
76	18	1.27	28	SH	
77				L	↑
78	20	1.21	35	SL	
79	28	1.06	68	SL	
82	14	1.34	22	SH	
84	17	1.45	28	SH	
86				L	↑
87	16	1.36	22	SH	
90	15	1.14	18	SH	↑
91	38	1.37	72	SH	
92	21	1.23	38	SP	↑
93	28	1.12	16	SH	
94	17	1.12	14	SH	
98	13	1.20	33	SH	↑
99	30	1.44	60	SH	
100	24	1.19	24	SH	
101				L	↑
102	60	1.42	92	SL	
103	16	1.46	35	SH	
104	14	1.35	34	SH	↑
105	51	1.12	45	SL	

1. Sample No.
2. Mode.
3. Sorting index.
4. Silt population (%).
5. Grain-size facies.
6. Grading.

similarities between stage 3 and the hypothermal stages 2 and 4 are consistent with the similarities of conditions (in particular the aeolian input regime) during these stages noted by Sarnthein *et al.* (1982).

TURBIDITIC DEPOSITION

The main part of the recovered sediments was ascribed to a regime of turbiditic emplacement (77 layers).

Some of the turbidite layers (Fig. 5) display a high benthic foraminifer content and low amounts of shelf-derived foraminifers, while others exhibit a high shelf-derived foraminifer content, sometimes associated with a high benthic foraminifer content. Two kinds of turbidites are thus portrayed, one corresponding to the reworking of sediment from the slope and the other indicative of a component provided by the shelf. The former occurrence seems predominant.

The samples whose turbiditic origin was established were grouped together in turbidite beds taking into account the variations in mode value, sorting index and silt population content. The increase in transport strength (duration and/or velocity) was directly responsible for an increase in central grain-size value, a decrease in the sorting index and/or an increase in population content. These criteria are clearly related to the graded sedimentation due to turbidity currents.

Altogether 43 turbidites were reported, generally coarsening upwards. They are interspersed within the pelagic layers (Tab. 4). The time distribution is shown Figure 8. In the interstage phases, turbiditic layers are only found during the cold to warm transitions and their attendant transgressions as observed by Faugères

et al. (1979) who evoked the reworking of shelf sediments during the sea level rise.

The $\delta^{18}O$ values of the turbidites display a fairly good agreement with the general trend of the hemipelagic $\delta^{18}O$ curve. Values are of the same order in stages 1, 3 and 5; however, stage 4 exhibits a strong discrepancy ($+0.86$ as an average in the hemipelagic record, $+0.33$ in the turbidite beds) and stage 2 is also higher with a difference of $-0.43\,^{0}/_{00}$ (average: 1.33 in hemipelagic layers, 0.90 in turbiditic layers). Fluctuations are generally higher in the turbidites during transitions between stages (4/3 and 2/1), when turbidites are strongly influenced by the previous stage values.

The frequency of turbiditic events discloses a major acceleration during the Holocene period (Tab. 5). The influence of a rapid succession of turbidites during the 2/1 transition is clearly responsible for the short average interval separating successive turbidites (700 years), but probably the time interval was shorter still during this transition (11 turbidite beds are located in the 2/1 transition and only three afterwards). There is no clear correlation between the presumed climatic trend and the period of turbiditic events, but it is noticeable that no turbiditic event occurred during the regression phases accompanying the 5/4 and 3/2 transitions.

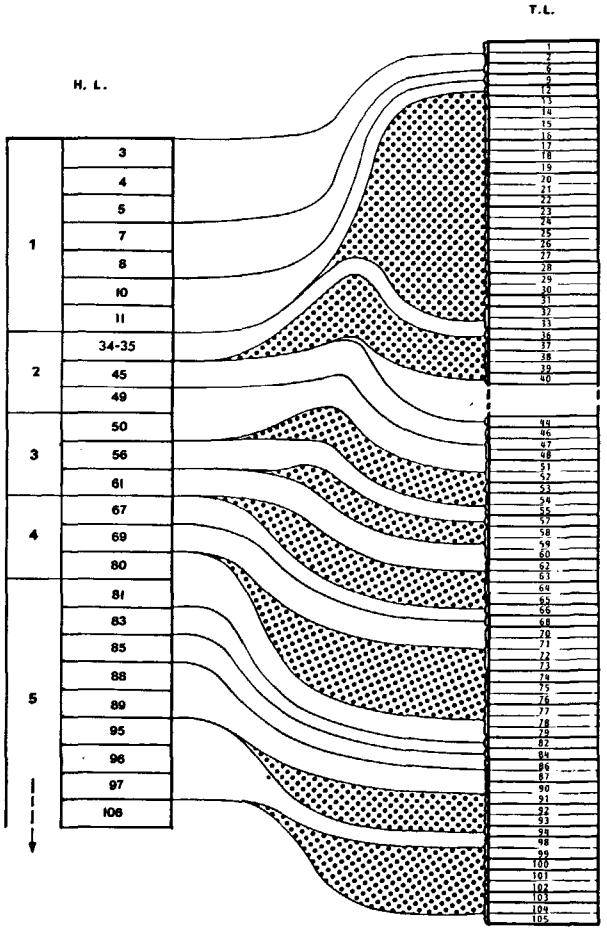

Figure 8

Stratigraphic relation between hemipelagic layers (HL) of the condensed stratigraphic column and turbiditic layers (TL).

Relations stratigraphiques entre les niveaux hémipélagiques (HL) du log réduit et les niveaux turbiditiques (TL).

Table 5

Number and periodicity of turbidites observed in the core M. 16401-4 *during the last* 125,000 *years.*

Dénombrement et périodicité des turbidites pendant les derniers 125 000 ans.

Isotopic stages	Number of turbidites	Duration of stage (ky)	T (ky)
1	14	10	0.7
2	5	18	3.6
3	8	34	4.2
4	5	13	2.6
5	11	$25 < t < 50$	2.3 to 4.6

CONCLUSION

The grain-size structure of the sediments of core 16401-4 frequently shows a silt population, usually unimodal, recognized as resulting from a sorting process. Only 29.2% of the layers show no evidence of such a silt population, of which 25 layers may be described as hemipelagic sediments considering their foraminiferal assemblage, isotopic values and carbonate content. Consequently, the others may be attributed to a turbidite deposition process and three grain-size criteria (mode value, sorting index and silt content) lead to the identification of 43 turbidites.

Carbonate content and isotopic ratios allow the subdivision of the condensed hemipelagic record by comparison with other dated stratigraphic columns from the region. The core bottoms in isotopic stage 5. The sedimentation rate for the hemipelagic component increased strongly during the Holocene period. Stage 3 is poorly represented.

Turbiditic events are most numerous during transitions from cold to warm periods. Changes in sea level, subsequent reworking of shelf sediments and also variations in pore pressure within slope sediments may have triggered off these turbidity currents. The Holocene interval is also characterized by higher turbiditic supply.

Acknowledgements

We wish to thank Michael Sarnthein, who invited one of us (J.P.B.) to participate in the Geotropex Cruise, offered his constructive criticisms of our first manuscript and encouraged us to pursue our investigations.

The laboratory work was funded by a grant from the CNRS (ATP Géologie et Géophysique des Océans).

We also wish to thank the Christian-Albrecht University (Kiel) for the facilities provided. We are particularly grateful to R. Zahn, who carried out the isotopic measurements. Lasten, we are indebted to an anonymous reviewer for his helpful suggestion concerning the out-of-phase variations of $\delta^{18}O$ and $CaCO_3$ signals.

REFERENCES

Berggren W. A., Hays J. D., Burckle L. H., Kennett J. P., Cita M. B., Opdyke N. D., Cooke H. B. S., Pastouret L., Funnell B. M., Gartner S., Shackleton N. J., Takayanagi Y., 1980. Towards a Quaternary time scale, *Quat. Res.*, **13,** 277-302.

Blanc-Vernet L., 1967. Contribution à l'étude des foraminifères de Méditerranée. Relations entre la microfaune et le sédiment. Biocoenoses actuelles, thanatocoenoses pliocènes et quaternaires, *Thèse Doct. État, Univ. Marseille,* 281 p.

Crowley J. J., 1983. Calcium carbonate preservation patterns in the central north Atlantic during the last 150,000 years, *Mar. Geol.*, **51,** 1-14.

Damuth J. E., 1975. Quaternary climate change as revealed by calcium carbonate fluctuations in western equatorial Atlantic sediments, *Deep-Sea Res.*, **22,** 725-743.

Ericson D. B., Ewing M., Wollin G., Heezen B., 1961. Atlantic deep-sea sediment cores, *Geol. Soc. Am. Bull.*, **72,** 193-286.

Faugères J.-C., Gayet J., Gonthier E., Grousset F., Latouche C., Maillet N., Poutiers J., Tastet J. P., 1979. Évolution de la sédimentation profonde au Quaternaire récent dans le bassin nord-atlantique : corps sédimentaires et sédimentation ubiquiste, *Bull. Soc. Géol. Fr.*, **21,** 5, 585-601.

Faugères J.-C., Gonthier E., Weber O., 1981. Signification des méthodes granulométriques pour la reconstitution des processus hydrodynamiques à partir de sédiments terrigènes carbonatés de milieux marins profonds, *Bull. Inst. Géol. Bassin Aquitaine,* **30,** 31-49.

Gardner J. V., Hays J. D., 1976. Responses of sea surface temperature and circulation to global climatic change during the past 200,000 years in eastern equatorial Atlantic, *Geol. Soc. Am. Bull.*, **145,** 221-246.

Griggs G., Kulm L. D., 1970. Sedimentation in Cascadia deep-sea channel, *Geol. Soc. Am. Bull.*, **81,** 1361-1384.

Hays J. D., Perruzza A., 1972. The significance of calcium carbonate oscillations in eastern equatorial Atlantic deep-sea sediments for the end of the Holocene warm interval, *Quat. Res.*, **2,** 355-362.

Kranck K., 1984. Grain-size characteristics of turbidites, in: *Fine-grained sediments: deep water processes and facies,* edited by D. A. V. Stow and D. J. W. Piper, Blackwell Scientific Publications, 83-92.

Lutze G. F., Pflaumann U., Weinholz P., 1986. Jungquartare Fluktuationen der benthischen Foraminiferenfaunen in Tiefsee-Sedimenten von NW-Afrika-Eine Reaktion auf Produktivitätsänderungen im Oberflächenwasser, *"Meteor" Forschungergebn.*, **40,** 163-180.

Martin R. T., Gadel F. Y., Barusseau J.-P., 1981. Evolution of Canet-Saint-Nazaire lagoon (Golfe du Lion, France) during the last stages of the Holocene, *Sedimentology,* **28,** 823-836.

Mienert J., 1986. Akustostratigraphie im äquatorialen Ostatlantik: Zur Entwicklung der Tiefenwasserzirkulation der letzten 3,5 Millionen Jahre, *"Meteor" Forschungergebn.*, **40,** 19-86.

Pflaumann U., 1975. Late Quaternary stratigraphy based on planktonic foraminifera of Senegal, *"Meteor" Forschungergebn.*, **23,** 1-46.

Pflaumann U., 1986. Sea-surface temperatures during the last 750,000 years in the eastern equatorial Atlantic: Planktonic foraminiferal record of "Meteor"-cores, 13519, 13521 and 16415, *"Meteor" Forschungergbn.*, **40,** 137-161.

Piper D. J. W., Normark W. R., 1983. Turbidite depositional patterns and flow characteristics. Navy submarine fan. California Borderland, *Sedimentology,* **30,** 681-684.

Rivière A., 1952. Sur la représentation graphique de la granulométrie des sédiments meubles, *Bull. Soc. Géol. Fr.*, **6,** 2, 145-154.

Ruddiman W. F., McIntyre A., 1967. Northeast Atlantic paleoclimatic changes over the past 600,000 years, *Geol. Soc. Am. Mem.*, **145,** 111-146.

Sarnthein M., Thiede J., Pfaumann U., Erlenkeuser H., Fütterer D., Koopmann B., Lange H., Seibold E., 1982. Atmospheric and oceanic circulation patterns off Northwest Africa during the past 25 million years, in: *Geology of the Northwest Africa continental Margin,* edited by U. von Rad, K. Hing, M. Sarnthein and E. Seibold, Springer Verlag, Berlin, 545-604.

Sarnthein M., Kögler F. C., Werner F., 1983. Forschungsschiff "Meteor" Reise Nr. 65 Aquatorialer Ostatlantik-Geotropex'83 Juni-August, 1983. Bericht der Wjissenschaftlichen Leiter, *Geol. Pal. Inst. Kiel, Berichte-Rep.*, **2,** 89 p.

Sarnthein M., Erlenkeuser H., von Grafenstein R., Schröder C., 1984. Stable-isotope stratigraphy for the last 750,000 years: "Meteor" core 13519 from the eastern equatorial Atlantic, *"Meteor" Forschungergebn.*, **38,** 9-24.

Van Zinderen Bakker E. M., 1967. Upper Pleistocene and Holocene stratigraphy and ecology on the basis of vegetation changes in subsaharan Africa, in: *Background to evolution in Africa,* edited by W. W. Bishop and I. Desmond Clark, Univ. Chicago Press, 125-147.